Journal of Rock Mechanics and Geotechnical Engineering 16 (2024) 1033–1048

Contents lists available at ScienceDirect

Journal of Rock Mechanics and Geotechnical Engineering

journal homepage: www.jrmge.cn

Full Length Article

A novel relationship between elastic modulus and void ratio associated with principal stress for coral calcareous sand

Ran Gao [a,b], Jianhong Ye [a,b,*]

[a] State Key Laboratory of Geomechanics and Geotechnical Engineering, Institute of Rock and Soil Mechanics, Chinese Academy of Sciences, Wuhan, 430071, China
[b] University of Chinese Academy of Sciences, Beijing, 100049, China

ARTICLE INFO

Article history:
Received 7 January 2023
Received in revised form
6 June 2023
Accepted 9 July 2023
Available online 7 September 2023

Keywords:
Coral calcareous sand (CCS)
Elastic shear modulus
Elastic bulk modulus
Triaxial test
Estimation formulation
Ye formulation

ABSTRACT

Elastic moduli, e.g. shear modulus G and bulk modulus K, are important parameters of geotechnical materials, which are not only the indices for the evaluation of the deformation ability of soils but also the important basic parameters for the development of the constitutive models of geotechnical materials. In this study, a series of triaxial loading-unloading-reloading shear tests and isotropic loading-unloading-reloading tests are conducted to study several typical mechanical properties of coral calcareous sand (CCS), and the void ratio evolution during loading, unloading and reloading. The test results show that the stress-strain curves during multiple unloading processes are almost parallel, and their slopes are much greater than the deformation modulus at the initial stage of loading. The relationship between the confining pressure and the volumetric strain can be defined approximately by a hyperbolic equation under the condition of monotonic loading of confining pressure. Under the condition of confining pressure unloading, the evolution of void ratio is linear in the e-lnp' plane, and these lines are a series of almost parallel lines if there are multiple processes of unloading. Based on the experimental results, it is found that the modified Hardin formulae for the elastic modulus estimation have a significant deviation from the tested values for CCS. Based on the experimental results, it is proposed that the elastic modulus of soils should be determined by the intersection line of two spatial surfaces in the G/K-e-p'/p_a space (p_a: atmosphere pressure). "Ye formulation" is further proposed for the estimation of the elastic modulus of CCS. This new estimation formulation for soil elastic modulus would provide a new method to accurately describe the mechanical behavior of granular soils.

1. Introduction

Elastic shear modulus G and elastic bulk modulus K are well known because they are essential measures of soil deformation ability and the fundamental parameters for the development of soil constitutive models. Numerous studies have been conducted on how these two moduli can be estimated. For example, Hardin and Richart (1963) and Richard et al. (1970) clearly found that the elastic shear modulus of soil was affected by the mean effective stress, void ratio, and the over-consolidation ratio, and they further suggested the earliest estimation formula for the elastic shear modulus as

$$G = G_0 \frac{(\psi - e)^2}{1 + e} p'^{\alpha} OCR^k \tag{1}$$

where G_0, ψ, α and k are the material-related dimensionless parameters; OCR is the over-consolidation ratio; e is the void ratio; and p' is the mean effective principal stress. Hardin and Richart (1963) suggested that $\psi = 2.17$ if the void ratio is in the range of 0.3–0.8 for the sand with rounded granular, and $\psi = 2.97$ if the void ratio is in the range of 0.6–1.3 for angular sand soil. It is easy to notice that the physical dimensions at both sides of Eq. (1) are inconsistent when the material parameter $\alpha \neq 1$. This is an obvious defect.

Subsequently, Seed and Shannon (1970) developed another estimation formulation for the elastic shear modulus of soils under small strain condition:

* Corresponding author. State Key Laboratory of Geomechanics and Geotechnical Engineering, Institute of Rock and Soil Mechanics, Chinese Academy of Sciences, Wuhan, 430071, China.
E-mail addresses: Yejianhongcas@gmail.com, Jhye@whrsm.ac.cn (J. Ye).
Peer review under responsibility of Institute of Rock and Soil Mechanics, Chinese Academy of Sciences.

https://doi.org/10.1016/j.jrmge.2023.07.011

$$G = 2.17K_{\max}p_a\left(\frac{p'}{p_a}\right)^{0.5} \tag{2}$$

where $K_{\max}$ is a dimensionless material parameter, and p_a represents the atmospheric pressure. The dimension at both sides in Eq. (2) is matched because of the introduction of atmospheric pressure. However, the effect of the void ratio is not considered in Eq. (2). Later, Iwasaki and Tatsuoka (1977) proposed a similar formula:

$$G = A(\gamma)B\frac{(2.17-e)^2}{1+e}p'^{n(\gamma)} \tag{3}$$

In Eq. (3), the introduction of Skempton's pore pressure coefficient B means that soil saturation was taken into consideration. The material parameters A and n are correlated with shear strain γ. Similar to Eq. (1), the physical dimension at both sides of Eq. (3) is not matched when $n(\gamma)\neq 1$. Furthermore, the specific expressions of $A(\gamma)$ and $n(\gamma)$ are difficult to be explicitly determined, resulting in that Eq. (3) being difficult to be used. Some scholars have also found that the factors, such as the coefficient of uniformity C_u (Menq et al., 2003), fine particles content F_c (Wang and Kuwano, 1999), mean particle diameter D_{50} (Hardin and Kalinski, 2005), and particle shape all have some effect on the elastic shear modulus of soil. However, the key influencing factors are still the void ratio e, as well as the mean effective principal stress p'. Since then, based on the work of Hardin and Richart (1963) and Richard et al. (1970), several scholars have made some minor corrections and improvements to these Hardin formulae. Several formulae for the estimation of elastic shear modulus which could only be applicable to some particular materials or under some special conditions (Wang and Zhang, 2007; Sun and Huang, 2011; Hu et al., 2011; Gao et al., 2013; Liu et al., 2017; Ovalle and Hicher, 2020) were further proposed, the most popular form is

$$G = G_0\frac{(2.97-e)^2}{1+e}\left(\frac{p'}{p_a}\right)^{\alpha} \tag{4}$$

where G_0 is a material parameter with the physical unit Pa, and α is a coefficient related to material property. Eq. (4) was referred to as the modified Hardin formula in the literature.

Hardin's formula actually is only an estimation formulation for the elastic shear modulus under the condition of small strain (generally less than 1%) involved in the resonance column test. Strictly speaking, the estimated results of the above Hardin's formula cannot be utilized in numerical modeling when a large deformation occurs. However, the elastic modulus of granular materials under large strain condition (>1%, even up to 35% which is impossible to be reached in the resonance column test) is an important parameter when forming the elastic stiffness matrix [$\boldsymbol{D}_e$] in numerical modeling under the classical framework of elasto-plastic theory, which will directly affect the reliability of computational results. However, there is still a lack of a reliable formula for the estimation of the elastic modulus under the condition of large strain. If Hardin's formula is used for the estimation of elastic modulus at large strain, it would inevitably lead to a large discrepancy with test results. Therefore, it is necessary to propose some new estimation formulations for the elastic modulus of soils under the condition of large strain. Moreover, these estimation formulae mentioned above are primarily applicable to terrestrial soils, e.g. quartz sand and river sand. It needs to be further explored whether they could be applied to the CCS widely existing in the marine environment.

Coral calcareous sand (CCS), also known as carbonate sand or coral sand (Coop, 1990), is composed of marine bioclastic sediments and is widely distributed in the South China Sea (SCS), Southeast Asia, the Middle East, the South Pacific Islands, and other areas, and it is a special geotechnical material with substantial differences from terrestrial soils. CCS has the characteristics of extreme angularity of particles shape, easily crashing, rough particles surface, and great friction angle. Its main mineral composition is calcium carbonate. CCS is the main material for the foundation of structures constructed on the reclaimed lands in the SCS. In recent decades, CCS receives considerable attention largely prompted by the exploitation of oil/gas in the offshore environment, such as the Australian North-West shelf, and by the civil infrastructure construction, e.g. the palm islands at Dubai in the United Arab Emirates, and these reclaimed lands on the top of natural coral reefs in the SCS. Many research works have been carried out on the mechanical properties of CCS, such as the quasi-static mechanical property (Coop, 1990; Coop and Atkinson, 1993; Porcino et al., 2008; He et al., 2021, 2022; Wang et al., 2022), dynamic property and liquefaction (Hyodo et al., 1998; Coop and Qadimi, 2007; Lopez-Querol and Coop, 2012; Xiao et al., 2018; Gao and Ye, 2019; Lv et al., 2019; Ding et al., 2021), bearing capacity (Wang et al., 2009, Wang et al., 2021b; Wan et al., 2021), creep behavior (Wang and Cai, 2017; Wang et al., 2018; Cao and Ye, 2019; Ye et al., 2019) and particles breakage (Coop et al., 2004; Donohue et al., 2009; Miao and Airey, 2013; Yu, 2018; Suescun-Florez et al., 2020; Cheng and Wang, 2021; Kuang et al., 2021; Lv et al., 2021; Wang et al., 2021a; Chen et al., 2022; Zhou et al., 2022). There are also some studies on the shear modulus of coral sand under small strain condition, such as Shi et al. (2021, 2022) and Giang et al. (2017). Furthermore, what they focused on in these previous works is generally the deformation modulus, rather than the elastic modulus. To the best knowledge, there are few studies on the elastic shear and bulk modulus of CCS, and their relationship with the void ratio and applied effective stress under large strain condition so far. At present, Eq. (4) is still occasionally used to estimate the elastic modulus of CCS under large strain condition. Unfortunately, the suitability of Eq. (4) has still not been verified for CCS under large strain condition. A series of triaxial loading-unloading-reloading shear tests and isotropic loading-unloading-reloading tests are performed in this study for the problem of the estimation of the elastic modulus of CCS. The CCS sampled from the SCS is used to prepare the test specimens. The elastic modulus can be measured from the stress-strain curves recorded during the elastic stage in the unloading-reloading process. By comparing the estimated values of the modified Hardin Formulae (Eq. (4) and (12)) with the measured results, the suitability of the modified Hardin Formulae for CCS could be checked.

Meanwhile, based on the experimental results, two new formulae are proposed in this study for the estimation of the elastic shear and bulk moduli of CCS. As a consequence, a new group of relationships between the elastic modulus, void ratio e, and the mean effective principal stress p' is successfully established. The comparative study shows that the new formulae established in this study have better estimation accuracy and more explicit physical meaning than the modified Hardin formula. It will offer a new idea for the development of constitutive models to describe the mechanical behavior of soils, especially for the CCS.

2. Materials and test plan

2.1. Material

The samples of CCS used in the test were all sampled from a reclaimed land in the SCS. At the engineering in-site, we performed more than 100 times of particle gradation tests and found that the grain size distribution (GSD) of the CCS varied significantly from

place to place on the reclaimed land. The average GSD of these test results at the in-site is selected as the representative in this experiment program, as shown in Fig. 1. The coefficient of uniformity $C_u = 6.18$ and the coefficient of curvature $C_c = 1.35$. The basic physical parameters of the CCS used in the test are listed in Table 1.

2.2. Specimen preparation

Eight hours of high-temperature dehydration and the subsequent natural cooling have to be done, to ensure the sand particles are completely dry. Then the coral sand samples are sieved and proportioned according to the GSD illustrated in Fig. 1b. The sand sample of each specimen was equally divided into seven parts and then poured into a cylindrical rubber membrane to make a cylindrical specimen with a diameter of 70 mm, and with a height of 140 mm. A suction cap in which a negative pressure has been generated is connected to the mold, making the rubber membrane tightly against the inner wall of the mold. The predetermined height (20 mm) of each layer is reached by the way of knocking. Since the compression process was done without a compaction hammer, only a very small amount of particle breakage would exist during the preparation. After the specimen has been made, the specimen average volume can be calculated by measuring the diameter of the top, middle and bottom of the specimen with vernier calipers, then the dry density of the specimen can also be obtained. If there is a large error with the target dry density, this specimen should be re-prepared.

2.3. Test plan and test instrument

All the tests are designed as the saturated drainage test, to reliably measure the volumetric strain of each specimen. Two parallel tests under the same condition are carried out to ensure the reliability of the test data. The dry densities of specimens are set as 1.45 g/cm^3, 1.55 g/cm^3, and 1.65 g/cm^3, respectively. The test plans are shown in Tables 2 and 3. It is known that 6 groups of isotropic loading-unloading-reloading tests, and 18 groups of triaxial loading-unloading-reloading shear tests will be conducted. All the tests are performed on the GDS DYNTTS equipment made in the UK. The measuring range of the load cell is 10 kN with an accuracy of 0.0001 kN. The measuring range of the piston-type volumetric controller is 250 mL with an accuracy of 0.001 mL. The DYNTTS equipment employed in the tests is shown in Fig. 2.

For the purpose of comparison and verification, four quartz sand specimens with two different dry densities, and with the same GSD of the CCS illustrated in Fig. 1b are prepared through artificial mixing. Among them, two specimens are for the isotropic loading-unloading-reloading test, and another two for the triaxial loading-unloading-reloading shear test. To ensure the comparability of the test results between CCS and quartz sand, the relative densities of the quartz sand specimens are set as same as the counterparts of CCS. Correspondingly, the dry density of quartz sand specimens is set as 1.78 g/cm^3 (medium dense state, $D_r = 46.7\%$) and 1.98 g/cm^3 (dense state, $D_r = 86.6\%$), respectively. The basic properties of the quartz sand are listed in Table 1, and the test conditions for the quartz and specimens are listed in Tables 2 and 3

Table 1
Basic physical parameters of CCS used in the test.

Soil	d_{60} (mm)	d_{30} (mm)	d_{10} (mm)	G_s	ρ_{max} (g/cm^3)	ρ_{min} (g/cm^3)
CCS	0.47	0.22	0.076	2.83	1.73	1.27
Quartz sand	0.47	0.22	0.076	2.65	2.06	1.59

Note: The quartz sand is Fujian standard sand, which is artificially prepared into the same GSD as CCS.

Table 2
Test conditions for the isotropic loading-unloading-reloading tests of confining pressure.

Test No.	Dry density (g/cm^3)	D_r (%)	Soil type	Drained	σ_3^u (kPa)	Parallel tests
I-1	1.45	46.7	Coral sand	Yes	100, 200, 400, 800, 1200, 1600, 1800	2
I-2	1.55	67.9			100, 200, 400, 800, 1200, 1600	2
I-3	1.65	86.6			100, 200, 400, 800, 1200, 1600	2
I-4	1.78	46.7	Quartz sand	Yes	100, 200, 400, 800, 1200, 1600, 1800	1
I-5	1.98	86.6			100, 200, 400, 800, 1200, 1600, 1800	1

Note: σ_3^u is the confining pressure at the unloading point. Furthermore, the target relative density D_r should be difficult to be reached with a resolution of 0.1% due to the unavoidable operation error during the preparation of specimens.

3. Experimental results and discussion

3.1. Elastic shear modulus

Typical stress-strain curves of the CCS and quartz sand with $D_r = 46.7\%$ recorded in the triaxial loading-unloading-reloading shear test are illustrated in Fig. 3. It is observed that the development trend of the stress-strain relationship during the unloading and reloading of deviatoric stress cannot radically be changed, and finally, the critical state can be eventually reached. The stress-strain

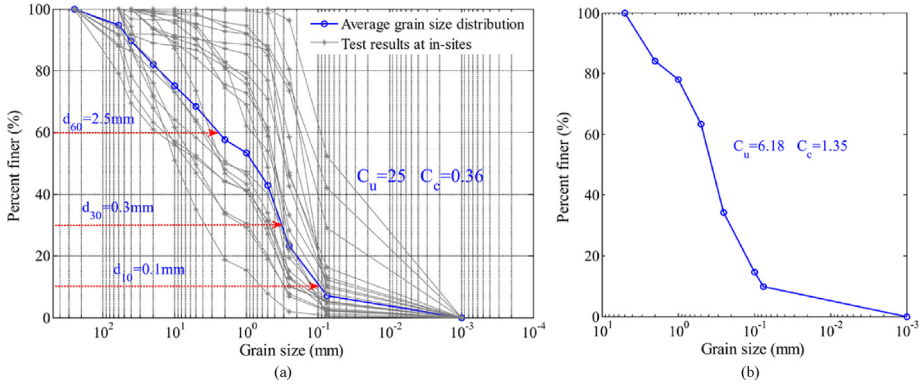

Fig. 1. The average GSD curve of the CCS used in this study: (a) Full particle size and (b) Used particle size less than 5 mm.

Table 3
Test conditions for the triaxial loading-unloading-reloading shear tests.

Test No.	Dry density (g/cm^3)	D_r (%)	Soil type	Drained	Confining pressure, σ_3' (kPa)	ε_1^u (%)	Parallel tests
T-1	1.45	46.7	Coral sand	Yes	200	3	1
T-2					200	5	1
T-3					200	7	1
T-4				Yes	400	3	1
T-5					400	5	1
T-6					400	7	1
T-7	1.55	67.9	Coral sand	Yes	200	3	1
T-8					200	5	1
T-9					200	7	1
T-10				Yes	400	3	1
T-11					400	5	1
T-12					400	7	1
T-13	1.65	86.6	Coral sand	Yes	200	3	1
T-14					200	5	1
T-15					200	7	1
T-16				Yes	400	3	1
T-17					400	5	1
T-18					400	7	1
T-19	1.78	46.7	Quartz sand	Yes	400	3, 5, 7	1
T-20	1.98	86.6			400	3, 5, 7	1

Note: ε_1^u is the axial strain at the unloading point.

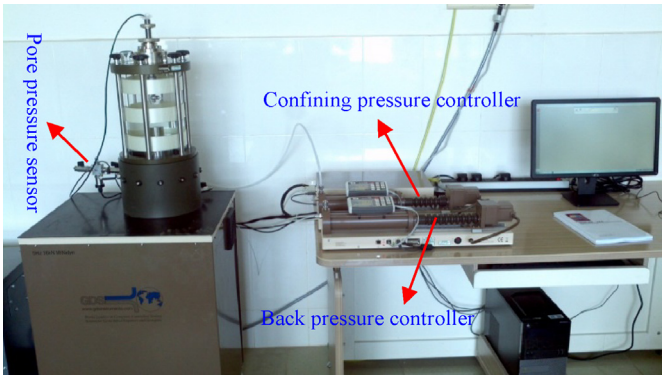

Fig. 2. The equipment DYNTTS employed in the test.

curves during several unloading stages are almost parallel with a great slope, and their slope slightly reduces at the end of each unloading stage. In Fig. 3a, it is also observed that each unloading curve and the corresponding reloading curve almost coincide, until the time when the plastic strain starts to be produced. After plastic strain is produced, the stress-strain curves at the unloading and reloading stage gradually separate. When the plastic strain is initially produced, the stress-strain relation gets into the elasto-plastic stage (marked as EP-S in Fig. 3a) from the elastic stage (marked as *E*-S in Fig. 3a). The corresponding point on the stress-strain curves is called the elasto-plastic separation point in this study, as marked by a series of short horizontal red lines in Fig. 3a. During the entire unloading-reloading process, it is found that the hysteresis loops are small or even absent. This characteristic is basically the same as that of quartz sand, but the area of these hysteresis loops of CCS is generally less than that of the counterparts of quartz sand.

This phenomenon implies that elastic deformation is mainly produced during the unloading and reloading processes, only a small amount of plastic deformation has been produced at this stage. Based on this recognition, Young's modulus E and Poisson's ratio ν can be determined in this study from the stress-strain relation recorded during the elastic unloading stage. The elastic shear modulus G and ν then can be calculated using the following formulae:

$$G = \frac{E}{2(1+\nu)} \tag{5}$$

$$\nu = \frac{\varepsilon_r}{\varepsilon_a} \tag{6}$$

where ε_r is the radial strain, and ε_a is the axial strain of specimens.

By substituting the void ratio e and the mean effective principal stress p' recorded during tests into the modified Hardin formula (Eq. (4)), the elastic shear modulus G of the CCS can be estimated. The comparison between the estimated value and the tested value is demonstrated in Fig. 4a, c and e. It is found that the value range of the estimated elastic shear modulus G adopting the modified Hardin formula (Eq. (4) is relatively narrow and the maximum estimated value is much less than the maximum measured value, while the minimum estimated value is greater than the minimum measured value. It is well illustrated by Fig. 4a, c and e that there is a significant discrepancy between the estimated values (marked as triangles) adopting the modified Hardin formula (Eq. (4)) and the measured values (marked as circles). Therefore, Eq. (4) is invalid for the estimation of the elastic shear modulus of CCS under the condition of large strain. Based on this recognition, it is not

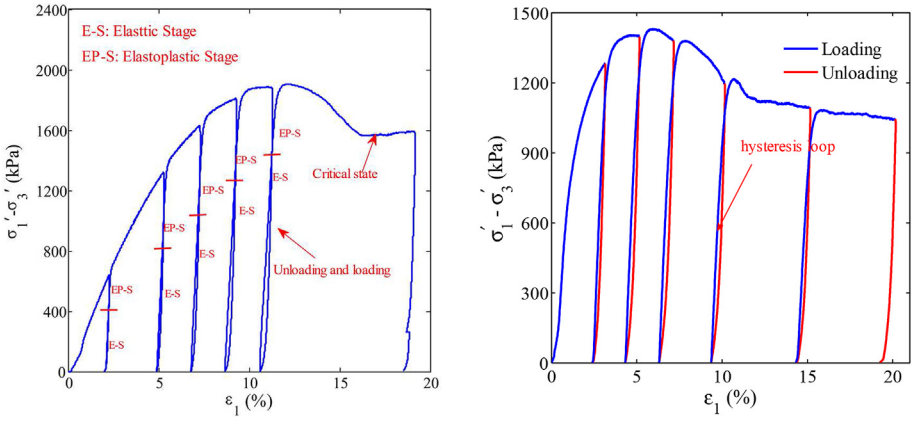

(a) CCS (D_r = 46.7%). (b) Quartz sand (D_r = 46.7%).

Fig. 3. Typical stress-strain relationship of CCS and quartz sand under the condition of deviatoric stress loading-unloading.

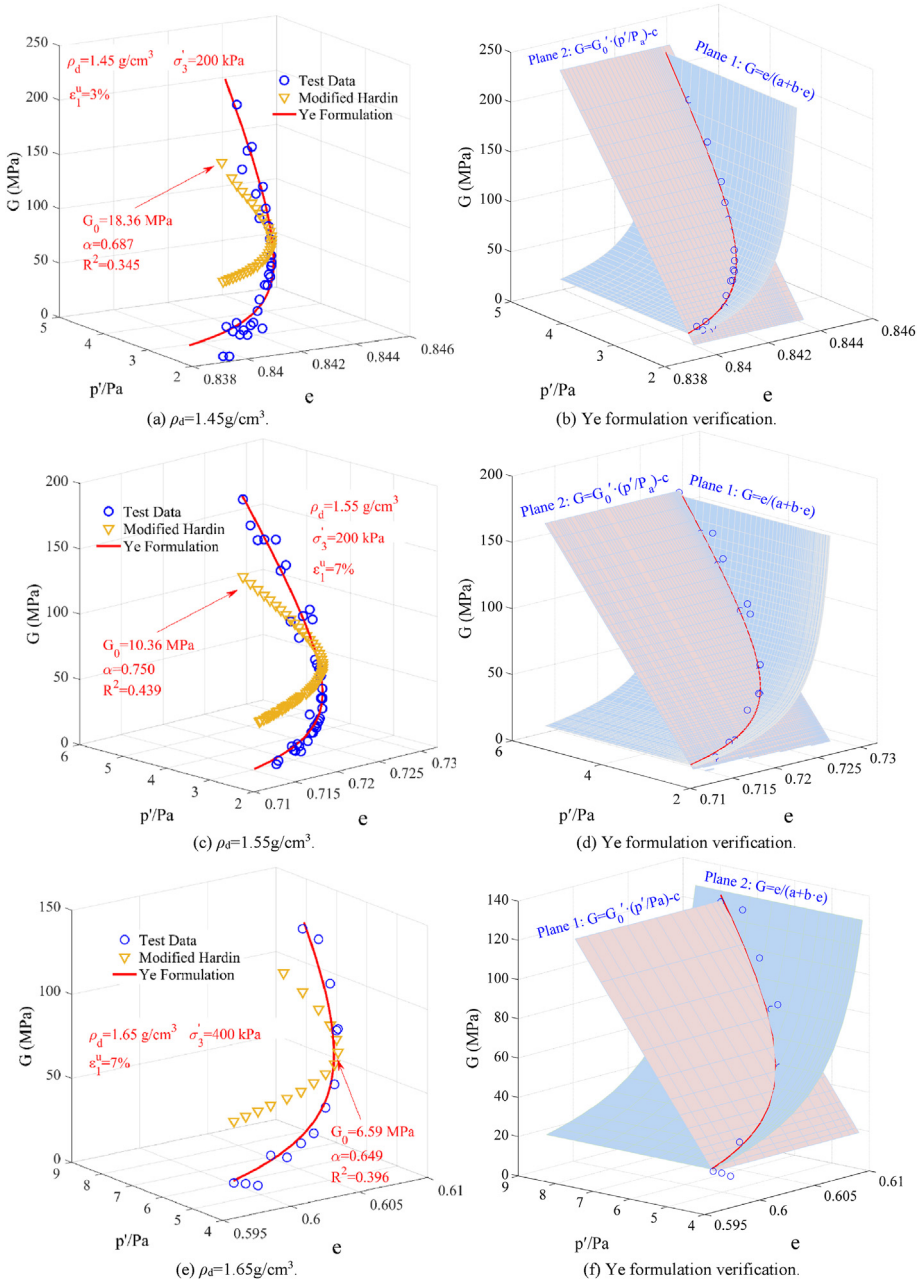

Fig. 4. Comparison and validation of the typical tested values of the elastic shear modulus of CCS with different estimation formulae.

recommended to adopt the modified Hardin formula (Eq. (4)) in the development of the constitutive models for CCS.

Since previous estimation formulae are not applicable to CCS, a new set of estimation formulae based on the experimental results will be proposed in this study. A large number of previous studies have shown that the void ratio e and mean effective principal stress p' are decisive influencing factors for the modulus estimation. Through comprehensive analysis of these test data, it is found that there is indeed a more explicit relationship among the elastic shear modulus G, void ratio e and p'. The relationship between them can be described by the following formula:

$$\left.\begin{aligned} G &= \frac{e}{a+be} \\ G &= G_0'\frac{p'}{p_a} - c \end{aligned}\right\} \tag{7}$$

where $p_a = 100$ kPa is the atmospheric pressure; and a, b, c and G_0' are the fitting parameters, depending on the dry density, applied confining pressure, as well as axial strain at unloading. In this study, this estimation formula is named 'Ye formulation' for the elastic shear modulus. It is shown by Eq. (7) that the relationship between the elastic shear modulus G and void ratio e is hyperbolic, and there

Table 4
Fitted values of a, b, c and G'_0 in the 'Ye formulation' for the G of CCS.

ρ_d (g/cm^3)	σ'_3 (kPa)	ε_1^u (%)	Ye formulation $G = \frac{e}{a+be}$			Ye formulation $G = G'_0\frac{p'}{p_a} - c$			Modified Hardin formulation $G = G_0\frac{(2.973-e)^2}{1+e}\left(\frac{p'}{p_a}\right)^{\alpha}$		
			a	b	R^2	G'_0 (MPa)	c	R^2	G_0 (MPa)	α	R^2
1.45	200	3	6.97	−8.26	0.95	83.72	155.8	0.94	18.36	0.687	0.345
		5	3.87	−4.57	0.89	54.09	101.9	0.99	10.53	0.822	0.394
		7	3.16	−3.89	0.95	59.7	120.3	0.95	8.79	0.855	0.342
	400	3	4.7	−5.86	0.85	69.33	239.7	0.85	14.88	0.763	0.391
		5	2.68	−3.51	0.85	54.6	176.8	0.82	9.02	0.951	0.532
		7	3.2	−4.03	0.94	46.41	162.7	0.92	8.44	0.899	0.525
1.55	200	3	3.36	−4.69	0.87	79.63	139.6	0.95	12.61	0.732	0.412
		5	2.86	−4.01	0.94	60.97	112	0.94	9.3	0.841	0.473
		7	1.977	−2.72	0.94	46.73	84.7	0.93	10.36	0.75	0.439
	400	3	11.53	−17.31	0.85	64.74	220.2	0.83	8.37	0.83	0.415
		5	2.21	−3.36	0.92	35.56	111.7	0.88	6.41	0.867	0.532
		7	1.937	−2.87	0.89	33.75	110.9	0.88	5.27	0.949	0.549
1.65	200	3	3.727	−6.13	0.95	57.6	99.8	0.95	10.43	0.602	0.342
		5	2.771	−4.54	0.93	56.08	103.9	0.93	7.86	0.689	0.321
		7	2.372	−3.66	0.99	49.78	95.36	0.98	6.73	0.816	0.373
	400	3	3.34	−5.83	0.91	39.58	97.95	0.88	8.32	0.782	0.519
		5	1.542	−2.67	0.92	34.74	100.3	0.88	7.16	0.813	0.548
		7	1.028	−1.68	0.96	27.98	91.9	0.93	6.59	0.649	0.396

is a linear relationship between the elastic shear modulus G and the mean effective principal stress p'. The fitted values of a, b, c and G'_0 for the experimental data adopting Eq. (7) are listed in Table 4.

It can be seen in Table 4 that it is credible to describe the physical relationship between G, e and p'/p_a by the hyperbolic and linear relationships formulated in Eq. (7), and the correlation coefficient R^2 is generally greater than 0.9 with a minimum of 0.82. While, the correlation coefficient R^2 from modified Hardin formula are mostly around 0.4. Therefore, it is implied that the elastic shear modulus of sandy soils can be estimated by adopting Eq. (7) in G-e-p'/p_a space with a better ability. In Table 4, one can see that the values of the parameters a, b, c and G'_0 exhibit a large dispersion. It is quite difficult for us to find some unified formulae to describe the relationship between the a, b, c, G'_0 and the dry density, applied confining pressure, as well as the axial strain at unloading. This dispersion for the values of a, b, c and G'_0 should be attributed to the inevitable test errors, as well as the high sensitivity of the a, b, c and G'_0 to the test data. Further research is needed in the future.

Further analysis on Eq. (7) confirms that the two equations in Eq. (7) describe a curved surface and a plane, respectively in G-e-p'/p_a space, as shown in Fig. 4b, d and f. The relationship among the elastic shear modulus of sandy soils G, e and p'/p_a in G-e−p'/p_a space is a spatial curve, and this spatial curve must be the intersection line between the curved surface and the plane described by the two equations in Eq. (7), as illustrated in Fig. 4b, d and f. The results shown in Fig. 4 have clearly demonstrated that the estimated results of the elastic shear modulus by Eq. (7) proposed in this study for CCS based on the concept of two surfaces intersection are more accurate and credible, compared with the modified Hardin formula (Eq. (4)).

3.2. Elastic bulk modulus

The typical stress-strain curves of CCS recorded in the isotropic loading-unloading-reloading test are shown in Fig. 5. It is observed in Fig. 5 that the unloading and reloading process of confining pressure cannot fundamentally change the development pattern of the confining pressure σ'_3 versus the volumetric strain ε_v. It means that the curves passing those initial unloading points in the σ'_3-ε_v coordinates basically are the same as that under monotonic loading. If the volumetric strain at unloading ε_v^u in the horizontal axis is normalized adopting the current void ratio e to eliminate the effect of dry density on the stress-strain relation, then the full process relationship of the confining pressure σ_3^u versus the volumetric strain ε_v^u/e can be approximately described by the hyperbolic equation under the conditions of isotropic consolidation compression, as demonstrated in Fig. 6. In this study, once a reloading curve and its previous corresponding unloading curve are initially separated due to the generation of plastic strain, the confining stress at this moment is expressed as σ_u. Meanwhile, the confining pressure at the beginning time of unloading is expressed as σ_3^u. It is found in Fig. 7 that the σ_u at the elastoplastic separation point is nearly half of the corresponding σ_3^u. That is to say, when the confining pressure at the reloading stage exceeds half of the corresponding σ_3^u in each unloading-reloading cycle, plastic deformation is produced again. As a result, the deformation of specimens gets into an elastoplastic stage from the elastic stage. The relationship between σ'_3 and ε_v at the unloading stage and subsequent reloading stage almost coincide before the applied σ'_3 is less than the corresponding $\sigma_3^u/2$. In the overlapping part, certainly there is only elastic deformation has been produced. There is an obvious phenomenon in Fig. 5 that the slope of the σ'_3-ε_v curves dramatically and gradually decreases when the applied σ'_3 is less than 200 kPa, regardless of at the unloading or reloading stage. Correspondingly, the elastic bulk modulus reduces rapidly. It is indicated that the elastic bulk modulus is highly dependent on the applied confining stress for soils.

It is observed from the typical stress-strain curves measured in the isotropic loading-unloading-reloading tests, shown in Fig. 5, that the greater the unloading confining pressure σ_3^u, the greater the bulk modulus at the initial unloading point, and the bulk modulus gradually reduces and eventually tends to 0 as the applied effective confining pressure decreases during unloading stages. It is indicated by this phenomenon that, like the elastic shear modulus, the elastic bulk modulus of soil represents a relationship with the mean effective principal stress p', which can be described by

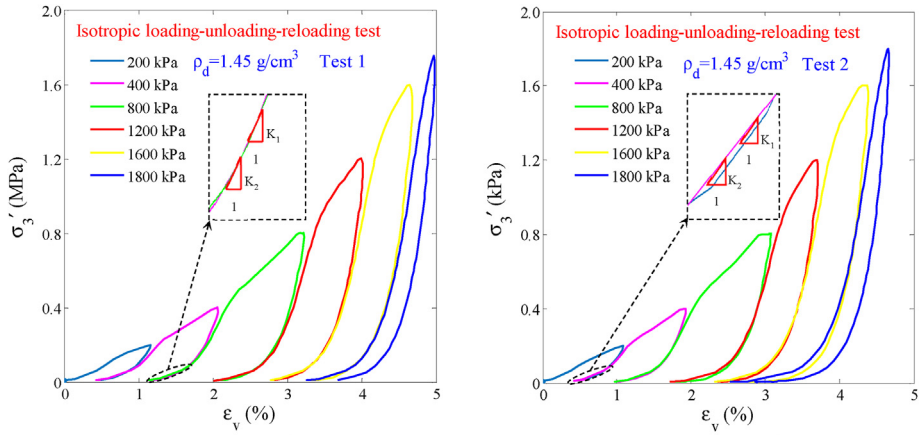

(a) CCS (ρ_d=1.45g/cm^3, Test 1). (b) CCS (ρ_d=1.45g/cm^3, Test 2).

Fig. 5. Typical stress-strain relationship of CCS recorded during the isotropic loading-unloading-reloading tests. Note: the elastic bulk modulus K is measured as the slope of the unloading and reloading σ_3'-ε_v curves when they are basically overlapped.

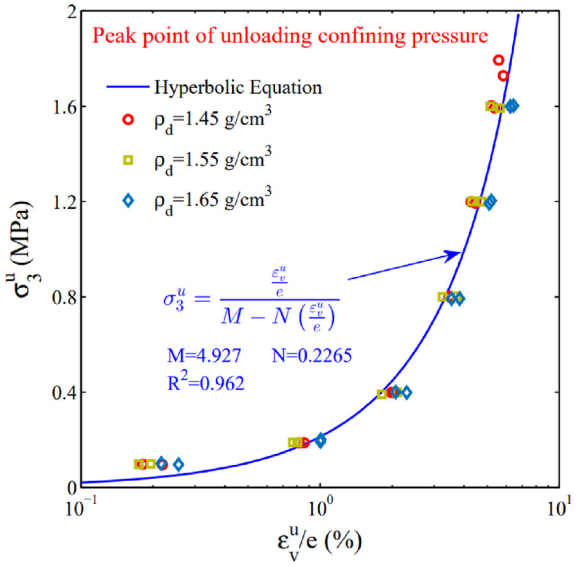

Fig. 6. Experimental relationship between the confining pressure at unloading σ_3^u and the corresponding normalized volumetric strain ε_v^u/e. Note: M and N are the fitting parameters.

$$K = K_0\left(\frac{p'}{p_a}\right)^m \tag{8}$$

where p_a = 100 kPa is the atmospheric pressure; K_0 is the elastic bulk modulus of soil when $p' = p_a$, which means that K_0 is a constant parameter without a relationship with p'; and m is a dimensionless fitting parameter. It is obvious that the dimension at both sides of Eq. (8) is matched perfectly due to the introduction of the atmospheric pressure p_a.

Here, a series of the elastic bulk moduli can be measured at the elastic deformation stage of each unloading-reloading cycle for each specimen, then the K_0 value of each specimen can be mathematically fitted adopting Eq. (8), as shown in Fig. 8. It is observed that there is a nearly perfect linear relationship between K and p'/p_a when the applied confining pressure is less than 800 kPa. It means that the dimensionless fitting parameter m = 1 is suitable for CCS. However, it is further surprised to find that the elastic bulk moduli of calcareous sand do not increase significantly when one specimen is unloaded from a high confining pressure (e.g. 1600 kPa), relative to that when the same specimen is unloaded from low confining pressure (e.g. 800 kPa). It was commonly believed that a specimen must be denser if it was isotopically compressed by higher confining pressure because the void ratio must reduce during the loading process, and a specimen with a less void ratio should have a greater elastic bulk modulus. Surprisingly, it is showcased in Fig. 8 that the elastic bulk moduli of calcareous sand measured at the elastic deformation stage during these reloading processes are basically on the same line for the same specimen. It seems that the elastic bulk moduli of calcareous sand are only linear with the applied confining pressure, regardless of whether the specimens are unloaded from a high or low confining pressure. It is indicated by this phenomenon that the main influencing factor for the elastic bulk modulus of calcareous sand is the applied mean effective stress and the individual effect of the void ratio is insignificant. The reason is that the relationship between the lnp' and void ratio e at the elastic deformation stage during the isotropic reloading process is linear in the lnp'-e coordinates (this characteristic will be presented thereafter). As a result, it is known

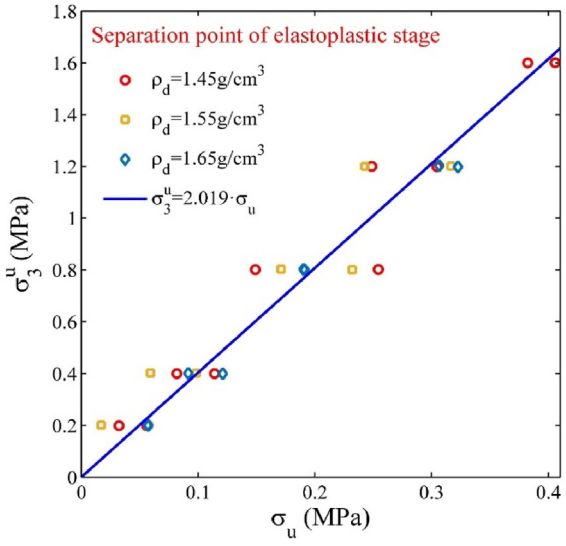

Fig. 7. Experimental relationship between the stress σ_u at the elastoplastic separation point and the corresponding confining pressure at unloading σ_3^u.

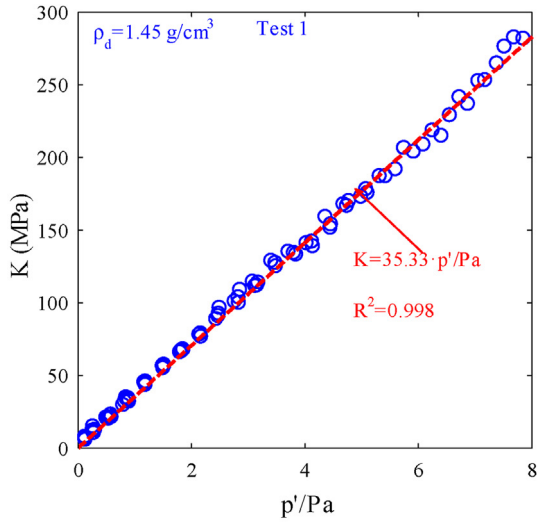

(a) K_0=35.33 MPa.

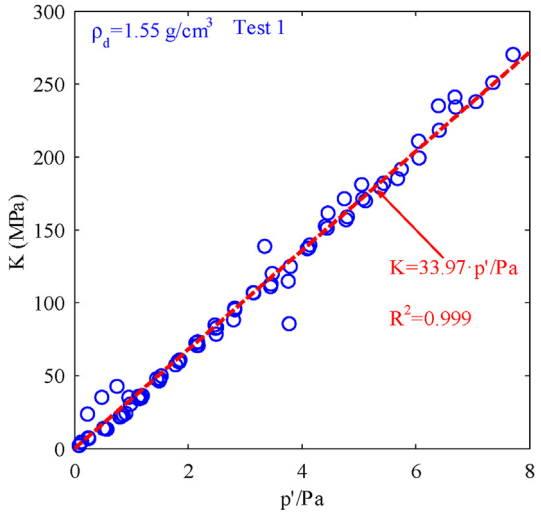

(b) K_0=33.97 MPa.

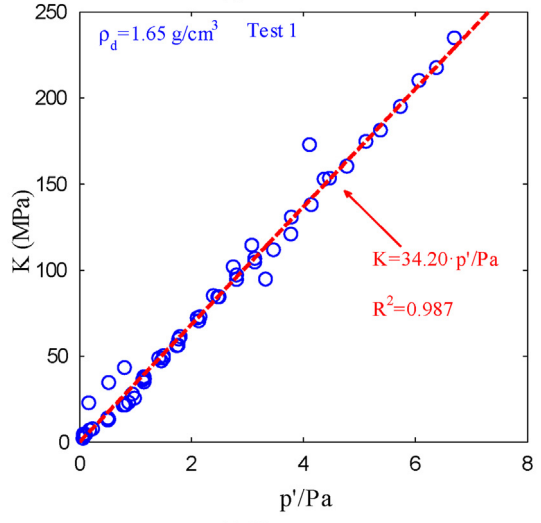

(c) K_0=34.20 MPa.

Fig. 8. Experimental relationship between the elastic bulk modulus and the mean effective principal stress for CCS.

that the void ratio e actually is the passive factor, and the applied mean effective stress is exactly the driving factor. Overall, the void ratio e is not an independent affecting factor for the elastic bulk modulus of calcareous sand.

All experimental data recorded in the isotropic loading-unloading-reloading tests are mathematically fitted adopting Eq. (8), and the fitted values of K_0 and m under each test condition are listed in Table 5. As can be seen in Table 5, the experimental data recorded in the isotropic loading-unloading-reloading tests can be described remarkably by Eq. (8), with the majority of R^2 greater than 0.99. It means that the reliability of Eq. (8) proposed in this study is good. Besides, it is found in Table 5 that the difference in the values of K_0 is insignificant under the condition of different initial dry densities, and there is no obvious relationship between the elastic bulk moduli and the dry density. It is indicated that K_0 is not sensitive to the initial dry density of the specimen, but should be closely related to the internal fabric of the specimen which is randomly formed in the process of specimen preparation. Due to the fact that the prepared specimens are impossible to be the same as each other from the perspective of the internal fabric, it is quite normal that the values of K_0 determined from parallel tests are slightly different.

3.3. Normal consolidation line

Generally, a normal consolidation line (NCL) is considered as an approximate bi-linear relationship in the $\ln p'$-e plane in the consolidation compression test for sandy soils in the field of critical state soil mechanics, taking the so-called pre-consolidation pressure as the transition point. The relationship between the void ratio e and the confining pressure p' of a NCL after the pre-consolidation pressure can be traditionally formulated by

$$e = e_\Gamma - \lambda \ln p' \tag{9}$$

where λ is the slope of the NCL, called as compression index; and e_Γ is the void ratio of soils when $p' = 1$ kPa.

It is commonly known that particle breakage cannot occur under medium and low confining pressures for silica sands because they have very high particle strength, and the compression index λ generally is constant. CCS, however, has the characteristics of particle angularity and lower particle strength. Fig. 9a, c and e shows the typical NCLs under isotropic consolidation condition for the CCS. It is found that these NCLs are not straight lines with a constant slope after the so-called pre-consolidation pressure, but are curves with a gradually increased slope. The increase of the slopes of NCLs is primarily due to the continuous particle crushing during isotropic consolidation. Before the initiation of particle crushing, the slopes of NCLs should be nearly constant. This phenomenon revealed here is the same as that observed by Coop, 1993 and Altuhafi and Coop (2011). The compression index of the CCS can be determined according to the increment of its void ratio and the confining pressure following $\lambda_p = -\Delta e/\Delta \ln p'$. The development of λ_p

Table 5
Fitting parameters for the relationship between the elastic bulk modulus and the mean effective principal stress for CCS.

Dry density (g/cm^3)	Estimation formulation $K = K_0(p'/p_a)^m$					
	Test 1			Test 2		
	K_0 (MPa)	m	R^2	K_0 (MPa)	m	R^2
1.45	35.33	1	0.998	37.12	1	0.999
1.55	33.97	1	0.999	33.36	1	0.995
1.65	34.2	1	0.987	41.92	1	0.992

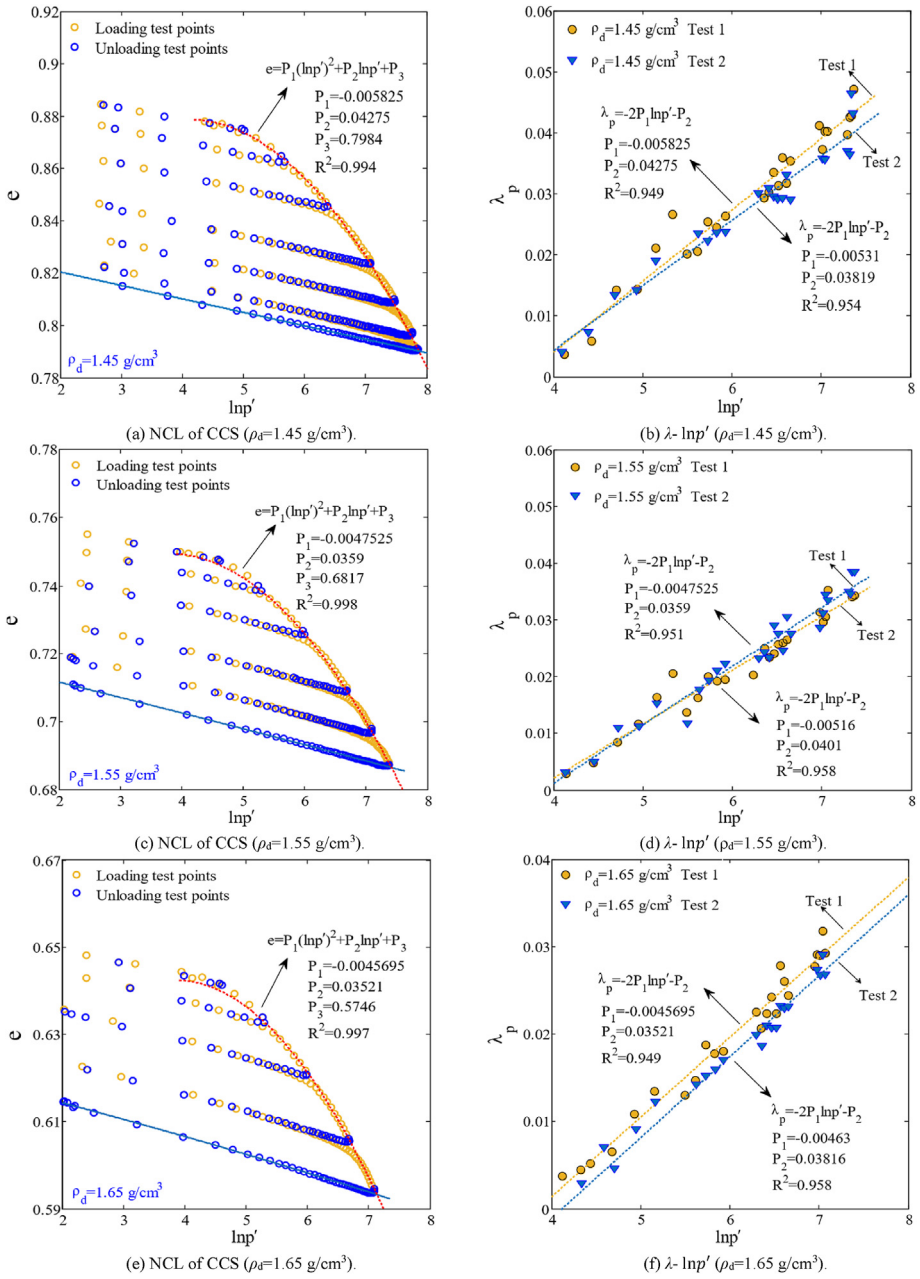

Fig. 9. Typical test relationship between the void ratio e, compression index λ and lnp' measured in the isotropic loading-unloading tests for CCS.

versus lnp' is illustrated in Fig. 9b, d and f. It can be seen that the NCLs of CCS are indeed not straight lines with constant slopes. The λ_p of NCL is positively related to the applied confining pressure. It is found that quadratic polynomials can describe these curved NCLs when involving particles crushing:

$$e = P_1(\ln p')^2 + P_2 \ln p' + P_3 \tag{10}$$

where P_1, P_2 and P_3 are three material-related parameters.

Due to the fact that the compression index is dependent on p', rather than a constant, the NCL could be rewritten as

$$e = e_\Gamma - \lambda_p \ln p' \tag{11}$$

where λ_p is the compression index where the confining pressure is p'. Comparing Eq. (11) with Eq. (10), it is known that $\lambda_p = -P_1 \ln p' + P_2$, and $e_\Gamma = P_3$ which is dependent on the initial dry density. As a consequence, Eq. (11) is formally consistent with the traditional expression of the NCL of sandy soils in which the compression index is constant. The compression index λ_p, however, is no longer constant but is related to the applied confining pressure, as illustrated in Fig. 9b, d and f. Obviously, the effect of the particle breakage of CCS on the NCL has been taken into consideration appropriately through the varied λ_p. It should be noted that the increase of λ_p should not be infinite. The increase of λ_p should stop at ultra-high confining pressure, as the particle breakage of CCS must cease when the granular material reaches its ultimate particle size gradation (Altuhafi and Coop, 2011), and the material will deform without further particle crushing.

Compared with that at the loading stage, the variation of void ratio is relatively simple during the unloading of confining

pressure. It can be seen in Fig. 9a, c and e that these unloading lines in e-ln (p'/p_a) plane appear as a set of approximately parallel linear clusters approximately with the same slope, which can be described by the following formula in the e-ln (p'/p_a) plane:

$$e = e_u - \lambda_u \ln\left(\frac{p'}{p_a}\right) \tag{12}$$

where λ_u is the slope of the unloading lines, and e_u is the void ratio when confining pressure is unloaded to $p' = p_a$ on the unloading line. As analyzed above, these unloading lines are approximately parallel, therefore, λ_u should be constant, rather than depend on confining pressure. Eq. (12) is used to mathematically fit the experimental data, and the fitted values of e_u and λ_u under different test conditions are listed in Table 6. It is shown that the descriptive ability of Eq. (12) is excellent because R^2 is all greater than 0.96. It can also be seen in Fig. 9a, c and e that the reloading lines are basically overlapped with the corresponding unloading lines in e-lnp' plane. It is indicated that there is no significant plastic deformation produced in these specimens during the unloading and the subsequent reloading process of confining pressure for the CCS.

The linear relationship between the elastic bulk module K and the mean effective principal stress p'/p_a has been described by Eq. (8). Eq. (12) also has plausibly described the linear relationship between void ratio e and ln (p'/p_a) during the elastic unloading stage. Then, the intersection lines of the two surfaces described by Eqs. (8) and (12) must represent the position of the elastic bulk modulus K in the three-dimensional space K-e-p'/p_a, as shown in Fig. 10b, d and f. Eqs. (8) and (12) are also referred to as 'Ye formulation' to form a group of formulae for the estimation of soil elastic modulus in this study. The modified Hardin formula for estimating the elastic bulk modulus of soil, similar to Eq. (4), is expressed as (Hu et al., 2018):

$$K = K_h \frac{(2.97 - e)^2}{1 + e}\left(\frac{p'}{p_a}\right)^{\beta} \tag{13}$$

where K_h is a material parameter with the unit of MPa.

Table 6
Fitted values of e_u and λ_u for the unloading lines under different test conditions (CCS).

Dry density (g/cm^3)	Confining pressure at unloading σ_3^u (kPa)	Estimation formulation $e = e_u - \lambda_u \ln(p'/p_a)$					
		Test 1			Test 2		
		e_u	λ_u	R^2	e_u	λ_u	R^2
1.45	100	0.8747	0.0042	0.99	0.8667	0.004	0.99
	200	0.8658	0.0044	0.98	0.8582	0.0045	0.99
	400	0.8521	0.0049	0.99	0.8456	0.0045	0.99
	800	0.8341	0.0051	0.99	0.8282	0.0052	0.99
	1200	0.8211	0.0051	0.99	0.818	0.0051	0.99
	1600	0.8102	0.0052	0.99	0.8084	0.0061	0.98
	1800	0.805	0.0052	0.99	0.8040	0.0062	0.99
1.55	100	0.7475	0.0035	0.99	0.7481	0.0033	0.99
	200	0.7414	0.0042	0.99	0.7413	0.0044	0.96
	400	0.7317	0.0044	0.99	0.7299	0.0043	0.99
	800	0.7184	0.0046	0.99	0.7143	0.0045	0.999
	1200	0.7079	0.0044	0.99	0.7041	0.0047	0.99
	1600	0.6997	0.0046	0.99	0.6948	0.0048	0.99
1.65	100	0.6414	0.0031	0.99	0.5976	0.0021	0.98
	200	0.6352	0.004	0.99	0.5921	0.0032	0.99
	400	0.6259	0.0037	0.99	0.5843	0.0032	0.99
	800	0.6139	0.0042	0.99	0.5729	0.0032	0.99
	1200	0.6038	0.004	0.99	0.5616	0.0034	0.99
	1600				0.5526	0.0034	0.99

The modified Hardin formula (Eq. (13)) is also used to mathematically fit the experimental data, the fitted values of K_h and β are listed in Table 7, and the comparison with measured values are shown in Fig. 10a, c and e. The comparison with the test data reveals that the estimated elastic bulk moduli adopting Eq. (13) is very closer to the experimental values. The fitted correction coefficient R^2 is generally greater than 0.9, but there is also a R^2 only equal to 0.59. Overall, the fitting result of the modified Hardin formula (Eq. (13)) is good. Nevertheless, this study would still not recommend the modified Hardin formula to be used for the elastic bulk modulus estimation, because the fitted values of K_h and β are different from case to case under different dry densities or different σ_3^u. Furthermore, it is quite difficult to establish an explicit relationship between K_h, β and the dry densities, as well as σ_3^u based on the data listed in Table 7. As a result, it will be very difficult to select the values of K_h and β under an arbitrary confining stress in numerical modeling. Taking the average for the values of K_h and β under different σ_3^u values for one dry density may be a feasible way. However, the discrepancy between the estimated K and measured values may also be difficult to be controlled. If Eq. (8) proposed in this study is used in numerical modeling, the K will be easily and reliably estimated, because the power index m is constantly equal to 1, and the coefficient K_0 is only related to the dry densities, as demonstrated in Table 5.

It should be noted that the variables e and p' are independent of each other in the modified Hardin formulae (Eqs. (4) and (13)). Each of the two formulae describes only one curved surface in the G/K-e-p'/p_a space. If the relationship between e and p' is not constrained by equations, e.g. Eq. (12), it can be assumed that the value of the elastic modulus of soil could be an arbitrary position on the surface. This obviously is not agreeable with the actual situation observed in the tests that the elastic modulus varies along some curved lines in the G/K-e-p'/p_a space (the experimental results have clearly revealed this feature).

The results shown in Figs. 4 and 10 have fully demonstrated the feasibility and accuracy of 'Ye formulation' for the estimation of elastic modulus. Compared with the modified Hardin formula, 'Ye formulation' has better credibility and suitability to a certain degree.

The fitted values of the parameters e_u and λ_u listed in Table 6 are only applicable to the corresponding initial dry density and the unloading confining pressure σ_3^u. To overcome this limitation, the fitted values of e_u and λ_u in Table 6 are normalized to explore the relationship between the parameters e_u, λ_u and the initial dry density and the unloading confining pressure σ_3^u. In this way, the application range of 'Ye formulation' (Eq. (12)) can be extended to any initial dry density and unloading confining pressure condition. By defining the state parameter $\Delta e = e_0 - e_u$ (e_0 is the initial void ratio), it is found that $\Delta e/\sqrt{e_0}$ and $\lambda_u/\sqrt{e_0}$ both have an exponential function relationship with the unloading confining pressure σ_3^u, as shown in Fig. 11. This exponential function can be described by

$$\frac{\Delta e}{\sqrt{e_0}} = 0.001103\left(\sigma_3^u\right)^{0.5753} \tag{14}$$

$$\frac{\lambda_u}{\sqrt{e_0}} = 0.002885\left(\sigma_3^u\right)^{0.08768} \tag{15}$$

3.4. Applicability to quartz sand

In the existing studies (Alikarami et al., 2015; Jafarian et al., 2018; Vranna et al., 2020), some experiments frequently are comparatively conducted on quartz sand to identify some unique

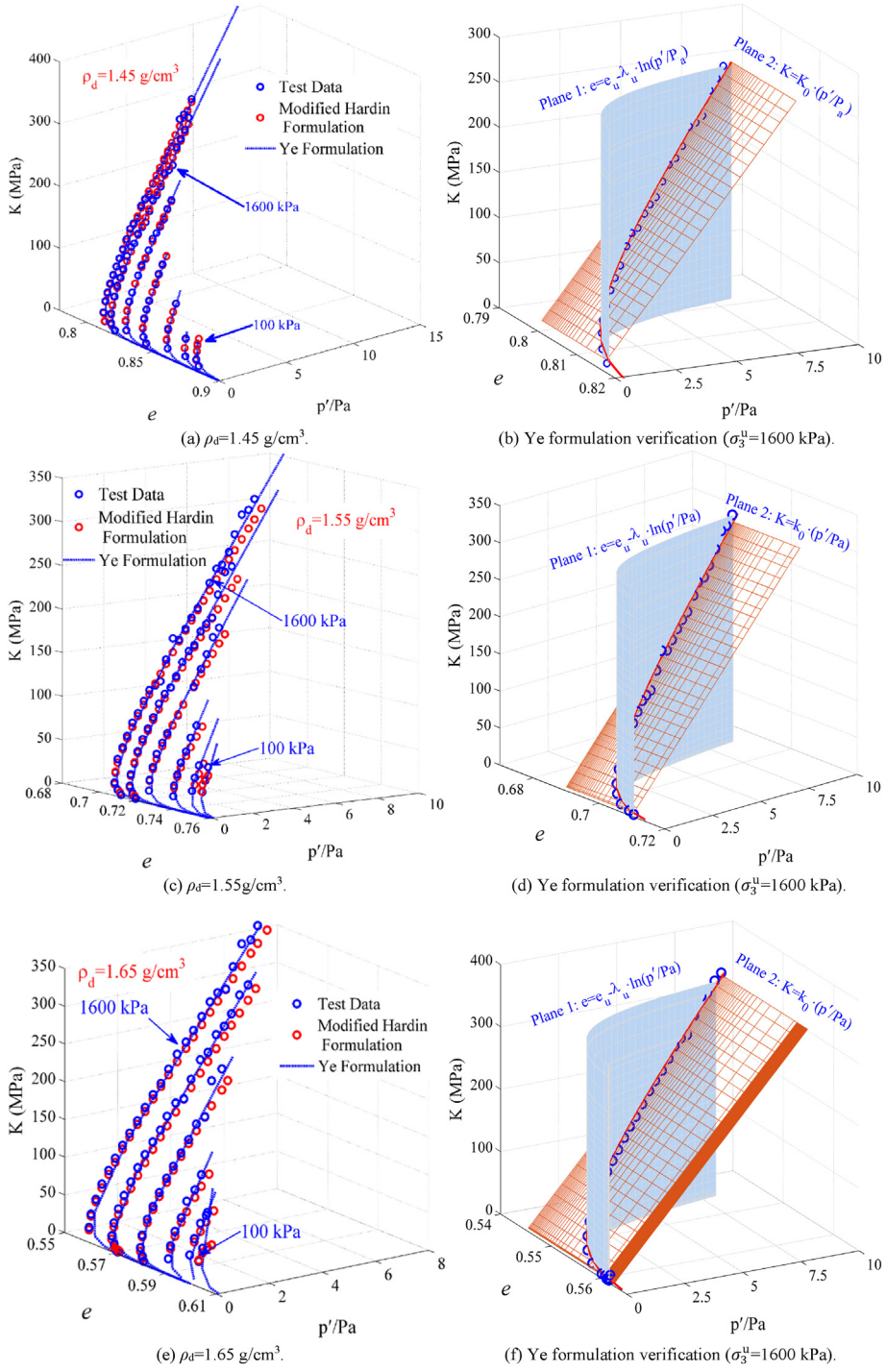

(a) ρ_d=1.45 g/cm^3. (b) Ye formulation verification (σ_3^u=1600 kPa).

(c) ρ_d=1.55g/cm^3. (d) Ye formulation verification (σ_3^u=1600 kPa).

(e) ρ_d=1.65 g/cm^3. (f) Ye formulation verification (σ_3^u=1600 kPa).

Fig. 10. Comparison and validation of the modified Hardin formula and 'Ye formulation' with typical experimental results.

behavior of CCS. In this section, to explore the applicability of the proposed 'Ye formulation' for the estimation of the elastic modulus of quartz sand, four quartz sand specimens with two different dry densities are prepared through artificial mixing, as mentioned in Section 2. Among them, Test Nos. I-4 and I-5 are for the isotropic loading-unloading-reloading test; meanwhile, Test Nos. T-19 and T-20 are for the triaxial loading-unloading-reloading shear test.

The experimental stress-strain relationships of quartz sand with D_r = 46.7% recorded in tests are illustrated in Fig. 12. Compared with that in Fig. 3, it is found that there is no essential difference in the triaxial loading-unloading-reloading curves between quartz sand and CCS. The only differences are that the peak shear strength and the corresponding axial strain of quartz sand are less than that of CCS, and the hysteresis loops between the unloading curves and the reloading curves of quartz sand are more obvious than that of CCS. Compared with that in Fig. 5, it is found that there is a significant difference between the two types of sands for the isotropic loading-unloading-reloading curves. In Fig. 12b, it is observed that the elastic volumetric deformation of quartz sand is considerable during the isotropic loading-unloading-reloading process. More

Table 7
Fitted values of K_h and β in the modified Hardin formula (Eq. (13)) for the K of CCS.

Dry density (g/cm^3)	Confining pressure at unloading σ_3^u (kPa)	Modified Hardin formulation $K = K_h \frac{(2.973-e)^2}{1+e}\left(\frac{p'}{p_a}\right)^{\beta}$					
		Test 1			Test 2		
		K_h	β	R^2	K_h	β	R^2
1.45	100	15.96	0.822	0.973	16.42	0.814	0.969
	200	15.11	0.855	0.998	16.54	0.962	0.989
	400	15.41	0.936	0.995	15.94	0.994	0.997
	800	14.89	0.962	0.998	15.89	0.961	0.995
	1200	14.85	0.94	0.998	15.67	0.939	0.995
	1600	13.68	0.992	0.996	15.36	0.962	0.975
	1800	14.1	0.972	0.997	15.23	0.95	0.994
1.55	100	14.09	0.306	0.627	11.69	0.185	0.799
	200	11.59	0.983	0.861	9.5	0.988	0.978
	400	12.36	0.899	0.943	12.37	0.807	0.832
	800	12.73	0.931	0.977	12.56	0.883	0.975
	1200	12.83	0.921	0.985	12.03	0.939	0.986
	1600	12.43	0.943	0.991	11.82	0.954	0.996
1.65	100	13.94	0.437	0.992	11.52	0.108	0.59
	200	10.47	0.852	0.884	12.89	0.728	0.78
	400	12.35	0.837	0.949	12.33	0.929	0.956
	800	11.51	0.895	0.924	12.45	0.968	0.974
	1200	11.36	0.908	0.989	11.14	1	0.996
	1600				12.09	0.952	0.994

than 70% of volumetric strain can recover with the reduction of the applied confining pressure. While considerable plastic deformation is generated for CCS under the same stress path.

Adopting the same measurement method for the elastic shear modulus and bulk modulus of CCS stated above, the elastic shear and bulk moduli of quartz sand are firstly measured. Furthermore, the modified Hardin formula and the proposed 'Ye formulation' are both utilized to mathematically fit these measured elastic moduli of quartz sand, as shown in Fig. 13. It is found that the estimated values of the modified Hardin formula under the condition of large strain are significantly different from the measured values (R^2 are all less than 0.5). It means this formula cannot be applied to the estimation of the elastic shear modulus of quartz sand. It is indicated by this result that the modified Hardin formula is only suitable for the elastic shear modulus estimation when a granular material is approximately ideally elastic under the condition of small strain, and the reliability of this formula will be significantly reduced when a granular material yields to produce plastic strain. However, the proposed 'Ye formulation' can better estimate the elastic shear modulus of granular materials under the condition of large strain, both for CCS and quartz sands. The fitting parameters are listed in Table 8.

The experimental relationship between void ratio e and mean effective principal stress lnp' of quartz sand recorded in the isotropic loading-unloading-reloading test is shown in Fig. 14. Compared with that in Fig. 9, it is found that the development tendency of e-lnp' for quartz sand has little difference from that of

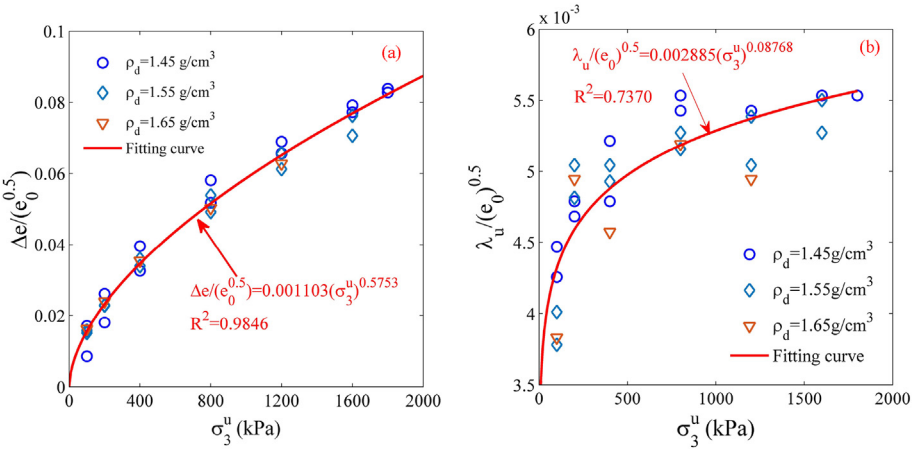

Fig. 11. Experimental relationship between e_u, λ_u and the initial void ratio e_0, σ_3^u.

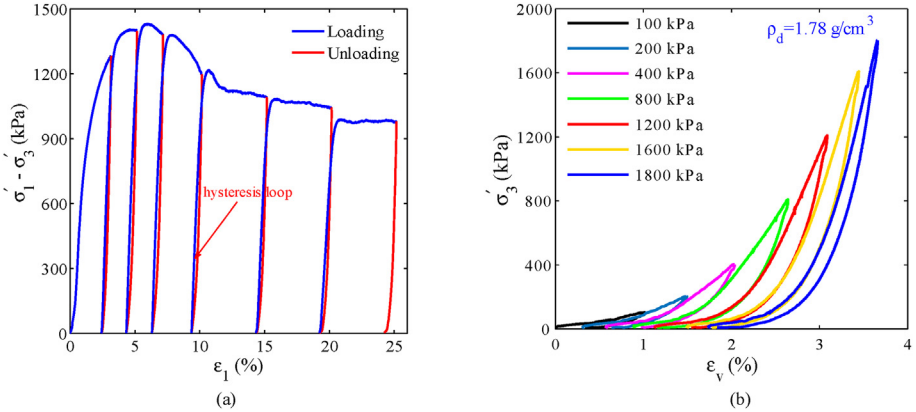

Fig. 12. Typical stress-strain curves of quartz sand (D_r = 46.7%): (a) Triaxial loading-unloading-reloading shear test, and (b) Isotropic loading-unloading-reloading test.

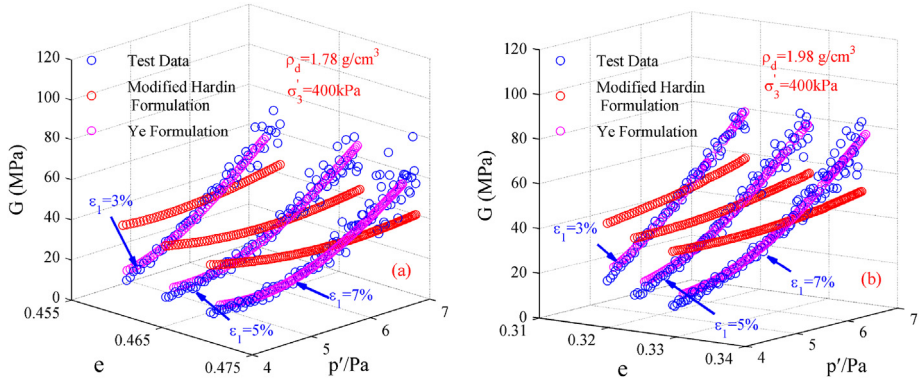

Fig. 13. Comparison and validation of the elastic shear modulus of quartz sand with different estimation formulations.

Table 8
Credibility comparison of the modified Hardin formula and 'Ye formulation' for quartz sand.

Dry density (g/cm^3)	Axial strain at unloading, ε_1^u (%)	Modified Hardin formula $G = G_0\frac{(2.973-e)^2}{1+e}\left(\frac{p'}{p_a}\right)^{\alpha}$			Ye formulation $G = \frac{e}{a-be}$		$G = G_a\frac{p'}{p_a} - c$		
		G_0	α	R^2	a	b	G_a	c	R^2
1.78	3	2.771	0.93	0.4836	0.7764	2.391	28.39	92.87	0.9773
	5	2.834	0.86	0.4485	0.5626	1.69	26.47	91.1	0.9613
	7	2.728	0.84	0.4182	0.5661	1.662	25.61	90.8	0.9591
1.98	3	3.382	0.71	0.4456	1.958	4.205	31.09	106.4	0.9181
	5	3.23	0.68	0.3937	1.409	2.975	28.25	99.63	0.9509
	7	3.15	0.64	0.3507	1.348	2.806	28.25	102.1	0.8994

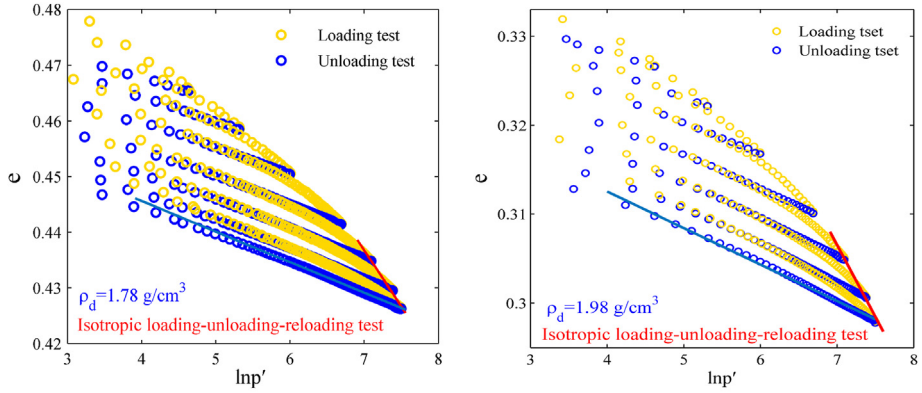

(a) NCL of quartz sand (ρ_d=1.78 g/cm^3). (b) NCL of quartz sand (ρ_d=1.98 g/cm^3).

Fig. 14. Typical experimental relationship between void ratio e and lnp' recorded in the isotropic loading-unloading-reloading tests for quartz sand.

CCS in general. The main difference is that the slope of the NCL of quartz sand basically remains constant since quartz sand particles have high particle strength and are not easy to break. However, the unloading lines in the e-lnp' space are also a series of straight lines, like that of CCS. Through mathematical fitting (as listed in Table 9), it is found in Fig. 15 that both the modified Hardin formula and the proposed 'Ye formulation' have good agreement on the estimation of the elastic bulk modulus of quartz sand.

Summarily, it is found through comparison and verification that the modified Hardin formula is only suitable for the estimation of the elastic bulk modulus of quartz sand and CCS. While 'Ye formulation' proposed in this study is suitable for the estimation of both the elastic shear and bulk moduli of quartz sand and CCS.

4. Conclusions

In this study, a series of triaxial loading-unloading-reloading shear tests and isotropic loading-unloading-reloading tests are conducted by taking the CCS sampled from the SCS as the test material. Based on the test results, a new set of formulae for the estimation of the elastic modulus of CCS, referred to as 'Ye formulation', is proposed. Through the analysis of the experimental results, the following findings are obtained in this study:

(1) It is observed that there is an obvious elastic deformation stage for CCS in the triaxial loading-unloading-reloading shear tests. The stress-strain curves at the unloading-reloading stage are almost overlapped before the

Table 9
Fitted values for the parameters in the modified Hardin formula and Ye formulation.

Dry density (g/cm^3)	Confining pressure, σ_3' (kPa)	Modified Hardin formula $K = K_h'\frac{(2.973-e)^2}{1+e}\left(\frac{p'}{p_a}\right)^{\beta}$			Ye formulation $e = e_u - \lambda_u \ln\left(\frac{p'}{p_a}\right)$		$K = K_0'\left(\frac{p'}{p_a}\right)^{\omega}$		
		K_h'	β	R^2	e_u	λ_u	K_0'	ω	R^2
1.78	100	7.601	0.7424	0.9201	0.4662	0.003251	32.83	0.88	0.9782
	200	8.134	0.7178	0.7042	0.462	0.003495			
	400	7.851	0.821	0.7936	0.4571	0.004437			
	800	7.426	0.9311	0.7899	0.4517	0.004542			
	1200	8.108	0.7844	0.8512	0.4476	0.004893			
	1600	9.431	0.8039	0.8252	0.4443	0.00515			
	1800	8.016	0.8362	0.8345	0.4416	0.005059			
1.98	200	8.328	0.8911	0.7434	0.3248	0.00233	39.94	0.85	0.9872
	400	8.034	0.6073	0.7634	0.3215	0.003028			
	800	9.121	0.7575	0.7937	0.3179	0.003505			
	1200	7.21	0.9151	0.8366	0.3148	0.003705			
	1600	8.002	0.8148	0.7744	0.312	0.003846			
	1800	6.684	0.904	0.7953	0.31	0.00398			

elastoplastic separation point has arrived, and the hysteresis loop is very small or even absent. In the triaxial shear tests, the unloading stress-strain curves are almost parallel to each other with a great slope. Only at the end of the unloading curves, the slope gradually becomes smaller and tends to 0 when the applied confining pressure becomes less and less.

(2) The confining pressure σ_3'-volumetric strain ε_v curve under the condition of confining pressure monotonic loading can be approximately described by a hyperbolic equation. During the unloading and reloading process of confining pressure, the stress at the elastoplastic separation point is about half of the corresponding unloading confining pressure σ_3^u. Since the particles of CCS have the characteristics of angular surface and easy breakage, the NCL is not a straight line with a constant slope, but a curve with an increasing slope which is positively related to the applied confining pressure. Based on the test results, it is found that the NCL of CCS can be described by a quadratic polynomial equation. Meanwhile,

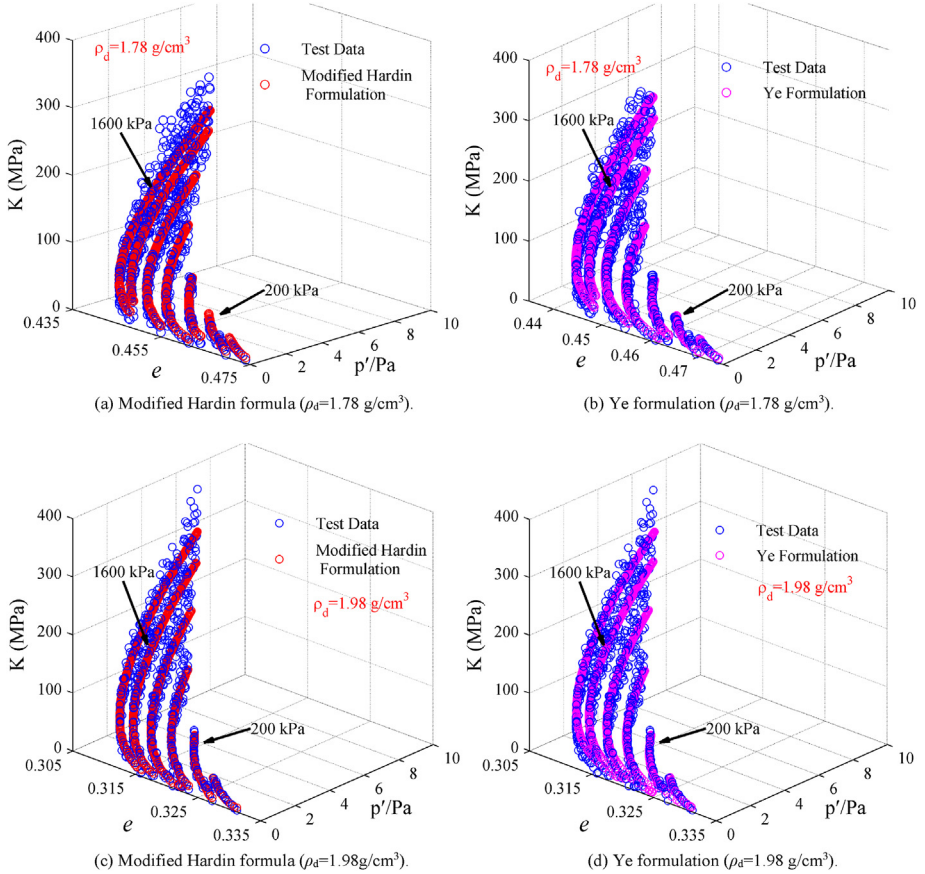

(a) Modified Hardin formula (ρ_d=1.78 g/cm^3). (b) Ye formulation (ρ_d=1.78 g/cm^3).

(c) Modified Hardin formula (ρ_d=1.98g/cm^3). (d) Ye formulation (ρ_d=1.98 g/cm^3).

Fig. 15. Comparison and validation of the elastic bulk modulus of quartz sand with different estimation formulations.

the unloading curves are presented as a series of approximately parallel linear clusters with a similar slope.

(3) Based on the experimental relationship between the elastic modulus (elastic shear modulus G and elastic bulk modulus K) and the void ratio e, mean effective principal stress p', a new group of formulae, referred to as 'Ye formulation', is proposed to estimate the elastic modulus of CCS. It is also proved that this group of new formulae have better reliability and suitability than the modified Hardin formulae. It is not recommended to use the Hardin estimation formula in the development of the constitutive models for CCS, due to its poor performance comparing with test data for the elastic shear modulus. The proposed 'Ye formulation' for the estimation of the elastic modulus of soil provides a new idea and method for the purpose of a more accurate description of the mechanical properties of soils, especially for CCS. It will have certain significance to the estimation of, as well as research on the elastic modulus of soils, especially sandy soils.

(4) Through comparative tests for CCS and quartz sand, it is confirmed that the modified Hardin formula is only suitable for the estimation of the elastic bulk modulus of quartz sand and CCS, while 'Ye formulation' proposed in this study is suitable for the estimation of both the elastic shear and bulk moduli of quartz sand and CCS.

Declaration of competing interest

The authors declare that they have no known competing financial interests or personal relationships that could have appeared to influence the work reported in this paper.

Acknowledgments

Professor Jianhong Ye is grateful for the funding support from the National Key Research and Development Program of China (Grant No. 2022YFC3102402).

List of symbols

G	Elastic shear modulus
Ψ, α, k	Material-related dimensionless parameters
OCR	Over-consolidation ratio of soil
e	Void ratio of soil
p'	Mean effective principal stress of soil
p_a	Atmospheric pressure
B	Skempton's B value, pore pressure coefficient
$A(\gamma)$, $n(\gamma)$	Material parameter correlated with shear strain γ
C_u	Coefficient of uniformity of soil
C_c	Coefficient of curvature of soil
F_c	Fines content of soil (%)
D_{50}	Mean particle diameter of soil
ρ_d	Dry density of soil
ρ_{max}	Maximum dry density of soil
ρ_{min}	Minimum dry density of soil
G_s	Specific gravity of soil particles
σ_3^u	Confining pressure at the beginning of unloading stage
σ_3'	Effective confining pressure
ε_1^u	Axial strain at the beginning of unloading stage
ε_r	Radial strain of soil
ε_a	Axial strain of soil
E	Young's modulus
ν	Poisson's ratio
a, b, c	Fitting parameters
ε_v	Volumetric strain of soil
ε_v^u	Volumetric strain at the beginning of unloading stage
σ_u	The stress at the elastoplastic separation point
K	Elastic bulk modulus
K_0	The elastic bulk modulus of soil when $p' = p_a$
λ	The slope of the NCL of soil
e_Γ	The void ratio of soils when $p' = 1$ kPa
P_1, P_2, P_3	Material-related parameters
λ_p	The compression index where the confining pressure is p'
λ_u	The slope of the unloading lines
e_u	The void ratio when confining pressure is unloaded to $p' = p_a$
R^2	Correlation coefficient
e_0	Initial void ratio of soil
Δe	Variation of void ratio

References

Alikarami, R., Andò, E., Gkiousas-Kapnisis, M., Torabi, A., Viggiani, G., 2015. Strain localisation and grain breakage in sand under shearing at high mean stress: insights from in situ X-ray tomography. Acta Geotech. 10, 15–30.

Altuhafi, F.N., Coop, M.R., 2011. Changes to particle characteristics associated with the compression of sands. Geotechnique 61 (6), 459–471.

Cao, M., Ye, J.H., 2019. Creep-stress-time four parameters mathematical model of calcareous sand in South China Sea, 1771-1178 Rock Soil Mech. 40 (5) (in Chinese).

Chen, S.S., Zhang, J.H., Long, Z.L., Kuang, D.M., Cai, Y., 2022. Effects of particle size on the particle breakage of calcareous sands under impact loadings. Construct. Build. Mater. 341, 127809.

Cheng, Z., Wang, J., 2021. An investigation of the breakage behaviour of a pre-crushed carbonate sand under shear using X-ray micro-tomography. Eng. Geol. 293, 106286.

Coop, M.R., 1993. The behaviour of granular soils at elevated stresses. Predictive soil mechanics. In: Proceedings of the Wroth Memorial Symposium, pp. 186–198. Oxford.

Coop, M.R., Sorensen, K.K., Freitas, T.B., Georgoutsos, G., 2004. Particles breakage during shearing of a carbonate sand. Geotechnique 54 (3), 157–163.

Coop, M.R., Qadimi, A., 2007. The Undrained cyclic behavior of a carbonate sand. Geotechnique 57 (9), 739–750.

Coop, M.R., 1990. The mechanics of uncemented carbonate sands. Geotechnique 46 (2), 357–362.

Coop, M.R., Atkinson, J.H., 1993. The mechanics of cemented carbonate sands. Geotechnique 43 (1), 53–67.

Ding, Z., He, S.H., Sun, Y.F., Xia, T.D., Zhang, Q.F., 2021. Comparative study on cyclic behavior of marine calcareous sand and tefrigenous siliceous sand for transportation infrastructure application. Construct. Build. Mater. 283, 122740.

Donohue, S., O'Sullivan, C., Long, M., 2009. Particle breakage during cyclic triaxial loading of a carbonate sand. Geotechnique 59 (5), 477–482.

Giang, P.H.H., Impe, P.O.V., Impe, W.F.V., Menge, P., Haegeman, W., 2017. Small-strain shear modulus of calcareous sand and its dependence on particle characteristics and gradation. Soil Dynam. Earthq. Eng. 100, 371–379.

Gao, R., Ye, J.H., 2019. Experimental investigation on the dynamic characteristics of calcareous sand from the reclaimed coral reef islands in the South China Sea. Rock Soil Mech. 40 (10), 3897–3908 (in Chinese).

Gao, Z., Zhao, J., Li, X.S., Dafalias, Y.F., 2013. A critical state sand plasticity model accounting for fabric evolution. Int. J. Numer. Anal. Methods GeoMech. 38 (4), 370–390.

Hardin, B., Kalinski, M., 2005. Estimating the shear modulus of gravelly soils. J. Geotech. Geoenviron. Eng. 131 (7), 867–875.

Hardin, B.O., Richart, F.E., 1963. Elastic wave velocities in granular soils. J. Soil Mech. Found Div. 89 (SM1), 33–65.

He, S.H., Shan, H.F., Xia, T.D., 2021. The effect of temperature on the drained shear behavior of calcareous sand. Acta Geotech. 16, 613–633.

He, H., Li, S.Y., Senetaki, K., Coop, M.R., Liu, S.Y., 2022. Influence of anisotropic stress path and stress history on stiffness of calcareous sands from Western Australia and the Philippines. J. Rock Mech. Geotech. Eng. 14 (1), 197–209.

Hu, W., Yin, Z.Y., Dano, C., Hicher, P., 2011. A constitutive model for granular materials considering grain breakage. Sci. China Technol. Sci. 54 (8), 2188–2196.

Hu, W., Yin, Z.Y., Scaringi, G., Dano, C., Hicher, P.Y., 2018. Relating fragmentation, plastic work and critical state in crushable rock clasts. Eng. Geol. 246, 326–336.

Hyodo, M., Hyde, A.F.L., Aramaky, N., 1998. Liquefaction of crushable soils. Geotechnique 48 (4), 527–543.

Iwasaki, T., Tatsuoka, F., 1977. Effects of grain size and grading on dynamic shear moduli of sands. Soils Found. 17 (3), 19–35.

Jafarian, Y., Javdanian, H., Haddad, A., 2018. Dynamic properties of calcareous and siliceous sands under isotropic and anisotropic stress conditions. Soils Found. 58 (1), 172–184.

Kuang, D.M., Long, Z.L., Ogwu, I., 2021. A discrete element method (DEM)-based approach to simulating particle breakage. Acta Geotech. 17, 2751–2764.

Liu, M.C., Zhang, Y., Zhu, H.Z., 2017. 3D elastoplastic model for crushable soils with explicit formulation of particle crushing. J. Eng. Mech. 143, 04017140.

Lv, Y.R., Li, X., Fan, C.F., Su, Y.C., 2021. Effects of internal pores on the mechanical properties of marine calcareous sand particles. Acta Geotech. 16, 3209–3228.
Lv, Y.R., Liu, J.G., Xiong, Z.M., 2019. One-dimensional dynamic compressive behavior of dry calcareous sand at high strain rates. J. Rock Mech. Geotech. Eng. 11 (1), 192–201.
Lopez-Querol, S., Coop, M.R., 2012. Drained cyclic behavior of loose Dogs Bey sand. Geotechnique 62 (4), 281–289.
Menq, F., Stokoe, K.H., Stephen, G.W., Rauch, A.F., Rathje, E.M., Bedford, A., 2003. Linear dynamic properties of sandy and gravelly soils from large-scale resonant tests. In: International Symposium on Deformation Characteristics of Geomaterials, pp. 63–71.
Miao, G., Airey, D., 2013. Breakage and ultimate states for a carbonate sand. Geotechnique 63 (14), 1221–1229.
Ovalle, C., Hicher, P.Y., 2020. Modeling the effect of wetting on the mechanical behavior of crushable granular materials. Geosci. Front. 11, 487–494.
Porcino, D., Caridi, G., Ghionna, V.N., 2008. Undrained monotonic and cyclic simple shear behavior of carbonate sand. Geotechnique 58 (8), 635–644.
Richard, F.E., Hall, J.R., Woods, R.D., 1970. Vibration of Soils and Foundations. Englewood Cliffs Prentice Hall, New Jersey, USA.
Seed, B.H., Shannon, I.M., 1970. Soil moduli and damping factors for dynamic response analyses. In: Technical Report No. EERC 70-10. College of Engineering, University of California, Berkeley, California, USA.
Shi, J.Q., Heageman, W., Cnudde, V., 2021. Anisotropic small-strain stiffness of calcareous sand affected by sample preparation, particle characteristic and gradation. Geotechnique 71 (4), 305–319.
Shi, J.Q., Xiao, Y., Wu, H.R., Liu, H.L., Heageman, W., 2022. Small-strain shear modulus of calcareous sand under anisotropic consolidation. Can. Geotech. J. 59 (6), 878–888.
Sun, H.Z., Huang, M.S., 2011. Critical state elasto-plastic model for coarse granular aggregates incorporating particle breakage. Chin. J. Geotech. Eng. 32 (8), 1284–1290 (in Chinese).
Suescun-Florez, E., Iskander, M., Bless, S., 2020. Evolution of particle damage of sand during axial compression via arrested tests. Acta Geotech. 15, 95–112.
Vranna, A., Tika, T., Papadimitriou, A., 2020. Laboratory investigation into the monotonic and cyclic behaviour of a clean sand stabilised with colloidal silica. Geotechnique 72 (5), 377–390.
Wan, Z.H., Dai, G.L., Gong, W.M., 2021. Study on the response of postside-grouted piles subjected to lateral loading in calcareous sand. Acta Geotech. 17, 3099–3115.
Wang, Y.S., Ma, L.J., Wang, M.Y., Lv, Y.R., Dong, L., Fan, P.X., 2018. A creep constitutive model incorporating deformation mechanisms for crushable calcareous sand. Arabian J. Geosci. 11, 1–8.
Wang, G.X., Kuwano, J., 1999. Shear modulus and damping of clayey sands. J. Earthq. Eng. 3 (2), 271–285.
Wang, G., Zhang, J.M., 2007. A cyclic elasto-plastic constitutive model for evaluating large liquefaction-induced deformation of sand. Chin. J. Geotech. Eng. 29 (1), 51–59 (in Chinese).
Wang, G., Wang, Z.N., Ye, Q.G., Zha, J.J., 2021a. Particle breakage evolution of coral sand using triaxial compression tests. J. Rock Mech. Geotech. Eng. 13 (2), 321–334.
Wang, Y.F., Cai, Z.Y., 2017. Experimental investigation of creep properties of saturated sand. J. Huaqiao Univ. Nat. Sci. 38 (1), 31–38.
Wang, X., Shan, Y., Cui, J., Zhong, Y., Shen, J.H., Wang, X.Z., Zhu, C.Q., 2022. Dilatancy of the foundation filling material of island-reefs in the South China Sea. Construct. Build. Mater. 323, 126524.
Wang, X.Z., Wang, R., Meng, Q.S., 2009. Laboratory load test of calcareous sand. Rock Soil Mech. 30 (1), 147–152 (in Chinese).
Wang, X.Z., Ding, H.Z., Meng, Q.S., Wei, H.Z., Wu, Y., Zhang, Y., 2021b. Engineering characteristics of coral reef and site assessment of hydraulic reclamation in the South China Sea. Construct. Build. Mater. 300, 124263.
Xiao, P., Liu, H.L., Xiao, Y., Studelein, A.W., Evans, T.M., 2018. Liquefaction resistance of bio-cemented calcareous sand. Soil Dynam. Earthq. Eng. 107, 9–19.
Ye, J.H., Cao, M., Li, G., 2019. Preliminary study on the creep characteristics of calcareous sand from reclaimed coral reef islands in South China Sea. Chin. J. Rock Mech. Eng. 38 (6), 1242–1251 (in Chinese).
Yu, F.W., 2018. Particle breakage in triaxial shear of a coral sand. Soils Found. 58 (4), 866–880.
Zhou, B., Ku, Q., Li, C., Wang, H., Dong, Y., Cheng, Z., 2022. Single-particle crushing behaviour of carbonate sands studied by X-ray microtomography and a combined finite–discrete element method. Acta Geotech. 17, 3195–3209.

Jianhong Ye is currently a full professor at the Institute of Rock and Soil Mechanics, Chinese Academy of Sciences (CAS). He obtained BEng from the China University of Geosciences (Beijing) in 2006, MEng from the Institute of Geology and Geophysics, CAS in 2009, and PhD from the University of Dundee in 2012. He accepted support from the National Overseas High-Level Talent Program in 2015. Over the last 15 years, he has developed the finite element software FssiCAS (http://www.fssi.ac.cn/download.html) for Fluid-Structure-Seabed Interaction (FSSI), ocean wave/seismic wave-induced dynamics and instability evaluation of marine structure and its seabed foundation. His research interests include marine geotechnics, soil liquefaction, FSSI and computational geomechanics. So far, he has published more than 60 high-level academic papers with over 1800 total citations (based on Google Scholar). He currently serves as an editorial board member of *Bulletin of Engineering Geology and the Environment*, *China Ocean Engineering*, *Rock and Soil Mechanics*, *Applied Sciences-Basel*, and *Geoenvironmental Disasters*. Prof. Ye has received several academic awards in China, and has been granted more than ¥20 million funding to support his research in the past 10 years.